MAUSAM, **54**, 1 (January 2003), 315-326

551.501 : 551.510.4

Satellite techniques for trace gas measurements

SHYAM LAL, VARUN SHEEL and PRABIR K. PATRA*

Physical Research Laboratory, Navrangpura, Ahmedabad-380009, India

**Frontier Research System for Global Change, Yokohama-2360001, Japan*

e mail : shyam@prl.ernet.in

सार – वायुमंडलीय गौण अवयवों का उपग्रह से मापन अत्यंत उपयोगी है क्योंकि ये लम्बे समय तक निरंतर भूमंडलीय व्याप्ति क्षेत्र उपलब्ध कराते हैं। तकनीकी विकास के फलस्वरूप क्षोभमंडल में भी ओज़ोन और अन्य संबद्ध ट्रेस गैसों का मापन पिछले दशक से संभव हो पा रहा है। नवीन प्रौद्योगिकी के आगमन से अवरक्त और सूक्ष्मतरंग में मापनों का उपयोग किया जा रहा है। तापमान और ओज़ोन के लिए क्रमशः उपग्रह से लिए गए प्रेक्षणों और पुनः प्राप्ति एलगोरिथ्म की ज्यामितियों को जानने के विभिन्न प्रकारों की उदाहरण सहित इसमें चर्चा की गई है। चूँकि भारत उपग्रहों के प्रक्षेपण की क्षमता रखता है अतः यह सुझाव है कि निम्न आनति वाले कक्षीय उपग्रह का उपयोग करके मौसम प्राचलों के साथ कुछ प्रमुख प्रदूषकों का मानीटरन करना महत्वपूर्ण होगा जिससे उष्णकटिबंधीय प्रदेश में उनके अंतरण और उनकी प्रक्रिया को समझा जा सके।

ABSTRACT. Satellite measurements of atmospheric minor constituents are very useful as they provide frequent global coverage over a long period of time. Due to technical developments measurements of ozone and other related trace gases are becoming possible since the past decade even in the troposphere. Measurements in the infrared and microwave are being utilised with the advent of new technology. Different types of viewing geometries of satellite observations and retrieval algorithms are discussed with examples for temperature and ozone, respectively. Since India is capable of launching satellites, it is suggested that monitoring some of the key pollutants along with meteorological parameters will be important to understand their transport and chemistry in the tropical region using a low inclination orbit satellite.

Key words – Ozone, Trace gases, Pollutants, Atmospheric transport, Satellite remote sensing, Viewing geometry, Radiative transfer, Retrieval algorithms.

1. Introduction

Ozone and related trace gases are very important to study atmospheric chemistry, radiation budget of the atmosphere and climatic change. Ozone, which is present only in small quantity (ppmv) in the atmosphere, has been known to absorb the lethal solar ultra violet radiation in the stratosphere (Brasseur and Solomon, 1986). Many anthropogenic gases containing halogens (Cl, Br, I) such as chlorofluorocarbons (CFCs) have been found to deplete this thin protective layer (Molina and Rowland, 1974). The other group of gases include biogenic gases like CO_2, CH_4, N_2O etc which also deplete ozone directly or indirectly (Crutzen, 1970) and are also important absorber of the earth's outgoing infrared radiation thereby causing global warming (Ramanathan *et al*., 1985). Abundances of many of these gases are increasing mainly due to growing industrial and agricultural needs. Measurements of these gases including ozone have become essential to monitor the changes, understand them and to predict their future impacts on climate change. Ground based techniques have been extensively used particularly for total ozone amount. However, for the measurements of the vertical distributions of ozone and other trace gases balloon or aircraft based techniques have been used (Subbaraya, 1987). But they provide limited spatial and temporal coverage. India Meteorological Department (IMD) conducts regular ozone soundings from Trivandrum, Pune and Delhi every fortnight. Vertical distributions of trace gases have been made using cryogenic air sampler flown on high altitude balloons from Hyderabad (Lal *et al*., 1996). However, the frequency of these measurements has been very poor due to high cost and also limited to a single place. On the other hand, satellites can provide almost global coverage and long term measurements. Figs. 1(a&b) show typical distributions of ozone on the vertical and horizontal planes.

The satellite measurements of trace species (chemical constituents as well as the aerosols) started in 1970s to study their global distribution and influence. However, routine measurements did not begin until 1978 with the launch of the Nimbus-7 satellite. Seven Nimbus spacecrafts were launched between 1964 and 1978 for testing atmospheric remote sounding instruments. The

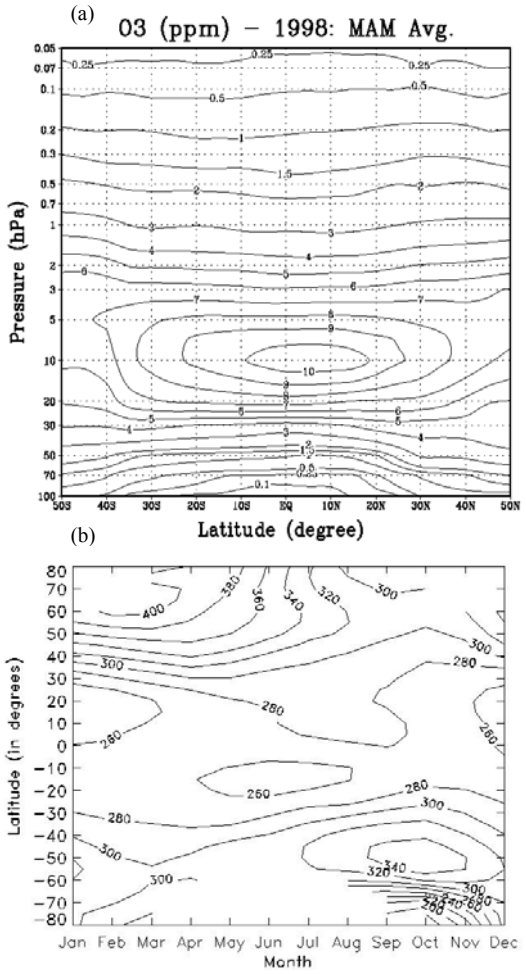

Figs. 1 a(&b). (a) A typical latitude-pressure distribution of O_3 mixing ratio (longitudinally averaged) as observed during March-April-May of 1998. This diagram is generated using the HALOE/UARS data produced by the analysis technique of Patra and Santhanam (2002) and (b) Month-latitude distribution of total columnar O_3 (in DU) measured by the TOMS instrument in 1990

instruments on board Nimbus 7 included the Total Ozone Mapping Spectrometer (TOMS), which measured total ozone and provided a large database to study various issues related to the ozone hole observed by Farman *et al*. in 1985. This was then used for deriving various parameters like spatial extent of ozone depletion in the northern and southern hemisphere (WMO, 1995). The low ozone values reaching down to about 100 DU (Dobson Unit, 1DU= $2.69*10^{16}$ mol/cm^2) have been observed in the SH and almost no ozone in the region of maximum ozone mixing ratio in the stratosphere (~20 km) during September-October months (Hofmann *et al*., 1994). The ozone hole for September 2000 is shown in Fig. 2. Since then TOMS or its variants are always in the space taking measurements.

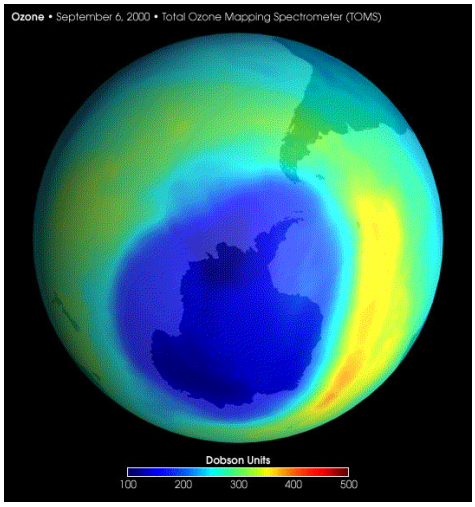

Fig 2. Dramatic O_3 depletion in Antarctica observed by TOMS in 2000

The global coverage of ozone has been also used to verify paradigms of stratospheric mean meridional transport. For instance the higher ozone levels in the middle and high latitudes than in the tropics (where ozone production is maximum) could be explained by ozone residence time and mean transport induced by the diabatic heating in the stratosphere (Garcia and Solomon, 1983) [Fig. 1(b)]. The photochemical lifetime of ozone in the stratosphere is longer than its transport lifetime. This is also the condition whether or not any specific trace gas can be useful for studying the dynamics of that particular layer of the atmosphere. Measurements of other trace species, such as methane (CH_4), nitrous oxide (N_2O) etc. were made by SAMS (Stratospheric and Mesospheric Sounder) in late 1970s. These measurements have been successfully utilized for studying the more complicated aspects of stratospheric dynamics in terms of propagation and breaking of planetary scale waves (Jones and Pyle, 1984).

One of the most exhaustive satellite measurement programme for trace gases has been the Upper Atmospheric Research Satellite (UARS), which was launched on 11 September, 1991 with as many as 10 instruments on board for measuring various dynamical, chemical and radiation parameters from upper troposphere to the top of the atmosphere. The primary focus however was on to explore the stratospheric ozone depletion chemistry and associated changes in the polar dynamics and radiation (Desseler *et al*., 1998 for a review). Since then several studies have been carried out by using the satellite measurements of trace species, such as O_3, CH_4, H_2O, N_2O etc., to study the dynamical characteristics of the stratosphere (Patra and Santhanam, 2002 and references therein). The temporal variabilities are also

becoming possible to study as the HALogen Occultation Experiment (HALOE) continued to collect observations till late 2001 (Patra *et al*., 2002). These variabilities are also being placed in juxtaposition to the high precision cryogenic air sampling experiment data (Patra *et al*., 2002a).

As the stratosphere is a stratified layer sitting over the troposphere, it was relatively simple to obtain global coverage multiple species distribution in this height region. The troposphere being closet to the ground, the change in air quality or pollution emission on the earth's surface and their transport to the neighbouring rather clean regions has started receiving utmost importance. By the end of 1980 some studies showed that ozone in the troposphere is increasing due to the enhanced pollution from biomass burning, automobile exhaust, and other industrial emissions. Ozone and related gases like CO, CH_4, NMHCs and their products in the troposphere and near the surface are important due to their role in climate change, and adverse effects on human health and crop. India Meteorological Department (IMD) has been making regular surface ozone measurements at many locations in India, but an extensive measurement plan has been operational by the PRL group to measure surface ozone and some of its precursors using state of the art analysers, to record their distributions and to understand the chemical processes involving ozone production, loss and transport (Lal *et al.*, 1998, 2000). These results for Ahmedabad while compared with 1954-55 measurement show an increasing trend of about 0.5%/year in surface ozone during this period (Naja and Lal, 1996). In 1991, Jack Fishman and coauthors showed ways to determine the amount of columnar tropospheric ozone from the total column data and stratospheric ozone from TOMS. They could clearly identify the regions of high ozone production caused by the African biomass burning and its transport to Atlantic Ocean (Fishman *et al*., 1991). Thereafter a couple of other techniques have been developed to estimate tropospheric ozone from the space; *e.g*., Ziemke *et al*. (1998) used the radiation reflection from the cloud tops, and Hudson and Thompson (1998) used a different trick for the same purpose.

To capture most of the tropospheric pollution events and regional emissions, the most recent trend is going towards more direct measurements of tropospheric constituents (*e.g*., CH_4, N_2O). The first in this series probably was the Interferometric Measurement of Gases (IMG) onboard the ADEOS (Advanced Earth Observing Satellite), funded by the National Aeronautics and Space Development Agency (NASDA, Japan). Though the ADEOS failed to complete the full measurement schedule due to technical difficulties (power failure), IMG has captured the tropospheric distribution of N_2O, CH_4, CO etc. in the period of August 1996 to February 1997. MOPITT (Measurements Of Pollutants In The Troposphere) was planned to put forward more focus on CO measurements. These measurements are currently serving as the first global database on CO distribution, primarily representing the middle troposphere (~500 hPa). The outflow of CO emission from the biomass burning in the Africa, South America, South-east Asia, North-east India are visible; however, the strength of emission is probably far from being estimated within a first order approximation.

On the same line, some focus is now diverted to measurement of carbon dioxide (CO_2) from the space. This poses a much harder problem by virtue of the fact that CO_2 radiation absorption properties are broadly overlapping with that of water (H_2O) in the Near-IR band and in the UV band. From the CO_2 emission estimation view point it is necessary to obtain information on its global distribution as close as possible to the ground. The observation of CO_2 near the ground by *in situ* or flask sampling is known to have spatial heterogeneity (Africa and South America are currently devoid of measurements) (Patra and Maksyutov, 2002). Thus observation from space is appearing to be the best potential to satisfy the global coverage for regional (sub-continental scale) surface source estimation with certain degree of confidence. Though the global CO_2 source estimation is well constrained, the regional flux can be constrained only longitudinally. In 2002, satellites have been launched which carry payloads capable of recording radiation spectra at high resolution so that retrieval of CO_2 distribution in the troposphere can be attempted. The SCIAMACHY was launched on board the Environmental satellite (ENVISAT) and AQUA on a NASA satellite (http://www.aqua.nasa.gov).

2. The radiative transfer equation

The radiation reaching a satellite carries energy which is detected by the sensors. The radiance or intensity (I or L) is defined as the radiant flux density per unit solid angle ($Wm^{-2}\ sr^{-1}$) and is wavelength dependent. The total radiance is the integral over all the wavelengths. Radiance is a useful quantity for satellite measurements, because it is independent of distance from an object as long as the viewing angle and the amount of intervening matter do not change. A blackbody is a perfect emitter (it emits the maximum possible amount of radiation at each wavelength) and also a perfect absorber. Planck derived the blackbody function $B_\lambda(T)$, describing the radiance emitted by a blackbody by the formula $B_\lambda(T) = 2hc^2\lambda^{-5}/[\exp(hc/\lambda kT)-1]$. It depends only on wavelength (λ) and temperature (T). The λ of maximum $B_\lambda(T)$ decreases with increasing temperature.

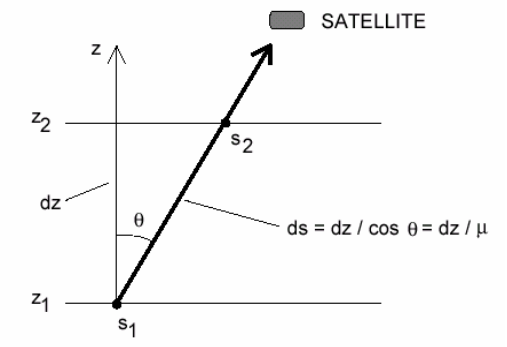

Fig. 3. Satellite geometry relative to source of emission (source: Strong, 2002)

All of the information received by a satellite about the earth and its atmosphere comes in the form of electromagnetic radiation. Therefore, we need to know how this radiation is generated and how it interacts with the atmosphere. The complete radiative transfer equation (RTE) can be derived for the transmission of radiation through the atmosphere by considering absorption, emission and scattering in the atmosphere. The RTE can be simplified in several ways to give versions that are very useful in remote sounding. One such assumption is neglecting clouds and scattering in the atmosphere. This is valid at infrared wavelengths because of $1/\lambda^4$ dependence of scattering. Assuming local thermodynamic equilibrium, we then get the Schwarzchild's equation, which describes the change in radiance I_λ as it travels through an atmospheric path of length ds and optical depth dδ.

$$\mu \frac{dI_\lambda}{d\delta_\lambda} = -I_\lambda(\mu,\varphi) + B_\lambda(T) \qquad (1)$$

where θ is the zenith angle and φ the azimuth angle as shown in Fig. 3. δ_λ is the optical depth from the surface to height z, *i.e* $\delta_{\text{vertical}}(0,z)$. The optical depth is defined as

$$\delta_{\text{slant}}(s_1,s_2) = \int_{s_1}^{s_2} n\ \sigma_e(\lambda,s)\,ds; \quad \delta_{\text{vertical}}(z_1,z_2) = \int_{s_1}^{s_2} n\ \sigma_e(\lambda,z)\,dz$$

$= \mu \times \delta_{\text{slant}}(s_1,s_2)$, where $\sigma_e = \sigma_a$ (absorption cross section) $+\sigma_s$ (scattering cross section), and n is the number density of the absorbing/scattering species.

The equation above can be integrated to calculate the radiance seen by a satellite instrument. For overhead viewing (θ=0, μ=1), the radiance reaching the satellite is given as

$$I_\lambda(S_{\text{sat}}) = I_\lambda(0)\tau_\lambda(0,\delta_{\text{sat}}) + \int_{\tau_\lambda(0,\delta_{\text{sat}})}^{1} B_\lambda(T)\,d\tau_\lambda \qquad (2)$$

TABLE 1

Details of wavelengths used for measuring various atmospheric gases

a. Ultra Violet (UV), Visible (VIS) and Infrared (IR) wavelength regions	
O_3	UV, VIS, 4.7μm, 9.6μm
N_2O	4.5μm, 7.8μm
CH_4	2.26μm, 3.3μm, 3.8μm, 7.7μm
CO	2.33μm, 4.7μm
CO_2	2.7μm, 4.3μm, 14.7μm
H_2O	6.3μm, 13.0μm
b. Microwave region	
118 GHz	*T*, *P*
190 GHz	H_2O, O_3, ClO, N_2O, HNO_3, SO_2
240 GHz	O_3, CO, *P*, *T*
640 GHz	N_2O, O_3, ClO, HCl, SO_2
2.5 THz	OH, P

P- Atmospheric Pressure, *T*- Atmospheric Temperature

Where the vertical transmission between optical depths δ_1 and δ_2 is defined as $\tau_\lambda(\delta_1,\delta_2) = \exp(-|\delta_1-\delta_2|)$. In the RTE above, the first term is the surface term and the second term is the black body atmospheric term integrated over different layers from surface to satellite. This equation is fundamental to the interpretation of satellite measurements of radiance in terms of atmospheric temperature and composition.

3. Remote sounding of temperature

We will first review the methods for temperature sounding, as the general principles are the same as that for remote sounding of atmospheric composition. Both use the fact that at any wavelength, atmospheric transmission is a function of temperature and mixing ratio of a gas that absorbs/emits radiation at that wavelength. Temperature is measured using a well-mixed gas (*e.g*., CO_2, O_2), whose mixing ratio is known and fairly constant with height. These measurements are done either in IR region (for CO_2) or in the microwave region (for O_2) where these gases have clear and strong absorption bands (Table 1). We use this temperature profile for a gas whose mixing ratio varies with altitude (*e.g*., O_3, H_2O), to retrieve it's mixing ratio from measurements of $I(\lambda)$ at absorption bands of the gas. In terms of sensitivity of the emission to a small change in temperature, 4.3 μm (CO_2 absorption band) is better for measuring warmer *T*, but 15 μm is still the best for lower *T*. So far, the 5 mm region (in the O_2 absorption band) emits the least energy and is least sensitive to temperature. However, the optimum wavelength for remote sounding of temperature is also determined by factors other than the available energy and the instrument sensitivity, such as the atmospheric transmission.

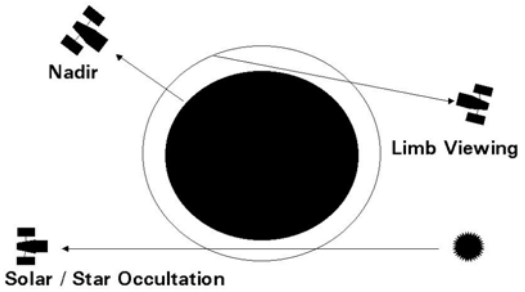

Fig. 4. Viewing geometries used in measurement of trace gases by satellites

3.1. *Nadir viewing or vertical sounding*

The satellite instrument looks vertically downwards in the [near] nadir direction, measuring radiation that leaves the atmosphere in the [near] local vertical. This viewing geometry provides a limited vertical resolution (Fig. 4 for viewing various viewing geometry). In the Schwarzchild's equation above, we introduce an altitude-dependent variable y, which can be z, p, $\ln(p)$, or any function monotonic in z (satellite is at height $z = z_1$):

$$I_\lambda(z_1) = I_\lambda(0)\tau_\lambda(0,z_1) + \int_{\text{surface}}^{\text{satellite}} B_\lambda(T)\frac{d\tau_\lambda}{dy}dy$$
$$= I_\lambda(0)\,\tau_\lambda(0,z_1) + \int_{\text{surface}}^{\text{satellite}} B_\lambda(T)\,K_\lambda(y)dy \quad (3)$$

Here $K_\lambda(y) = d\tau_\lambda/dy$ is called a weighting function. Often, $y = -\ln(p)$ to make $K_\lambda(y)$ more nearly independent of temperature.

A nadir-viewing instrument thus sees a surface term and an atmospheric term which is the integral of the blackbody emission from each layer weighted by $K_\lambda(y)$. We can determine the form of $K_\lambda(y)$ by considering the lower atmosphere (< 40 km) where Lorentz (collisional) broadening dominates for absorption lines in molecular bands. Choosing a single frequency ν in the wing of a collisional broadened spectral line, one can derive the weighting function as $K_\nu(y) = 2(p/p_{max})^2 \exp[-(p/p_{max})^2]$, (Houghton *et al*., 1984) where $y = -\ln(p)$, p is the pressure and p_{max} is the pressure at which $K_\nu(y)$ is maximum. This function is plotted in Fig. 5.

A vertical profile of temperature can be obtained by choosing an appropriate weighting function. Because K_ν varies with ν, different ν will possess weighting functions that peak at different heights. By measuring the intensities at a series of ν, a range of altitudes will be represented. Observations in the wings of a Lorentz line (where there is less absorption) will see deeper into the atmosphere, while observations closer to line centre (with maximum absorption) will see only the top layers of the atmosphere. This can be seen in Fig. 6 which shows the transmittance (left panel) and weighting functions (right panel). The contribution of the surface emission term will be reduced if the transmission is small, *i.e*., if the observation is not being made in an atmospheric window. The atmospheric emission term includes information on the temperature through the blackbody function, and on both the temperature and the concentration profile of the absorbing/emitting gas through the transmission and hence through the weighting function.

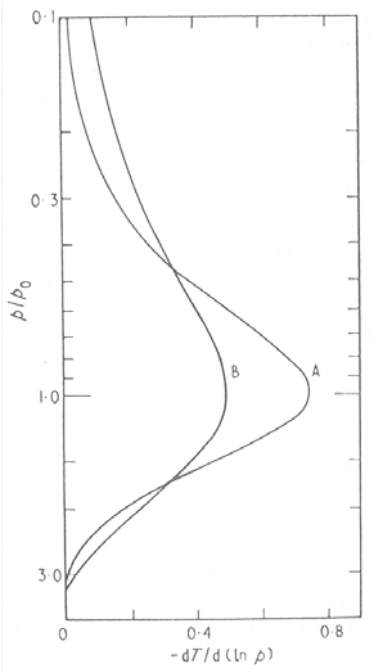

Fig 5. Weighting functions for : A, a monochromatic frequency in the wing of a collision broadened line; B, a strong Elsasser band (Houghton *et al*., 1984).

3.2. *The limb sounding technique*

The satellite instrument looks towards the limb (horizon) of the atmosphere, measuring radiation that leaves the atmosphere nearly tangentially (Fig. 4). Here the same radiative transfer equation is used, but for a different geometry. We no longer have a surface term and the intensity is integrated along the limb viewing line-of-sight.

The advantages of limb sounding are: (*i*) Good vertical resolution because the weighting functions peak sharply at the tangent height, with the instrument seeing nothing below $Z_{tangent}$ (tangent height, the height above the

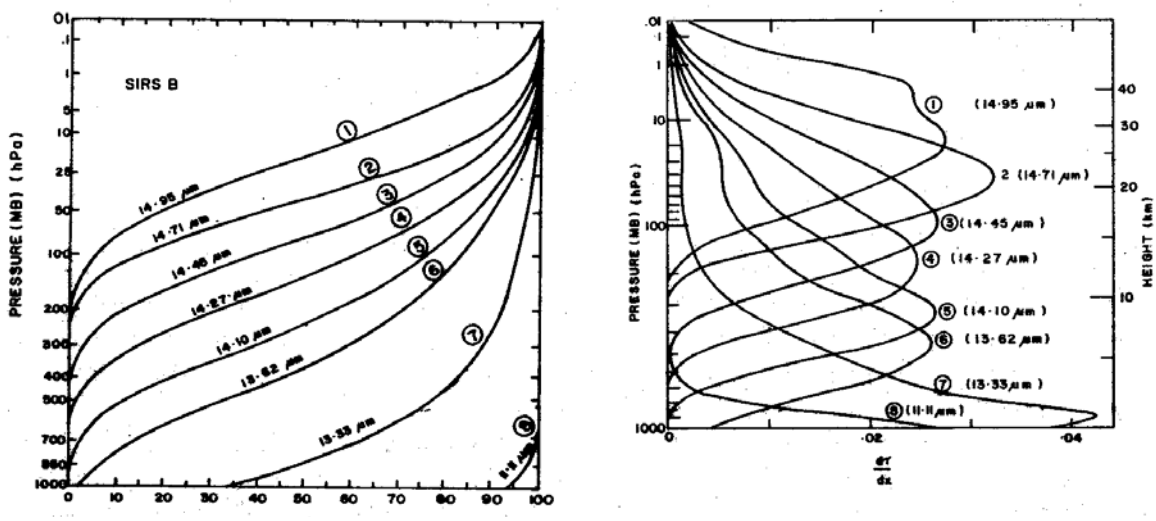

Fig. 6. Transmittance and weighting functions of 8 channels of CO_2 in SIRS (Yates, 1972)

surface of the closest point to the Earth in the instrument's line-of-sight) while pressure and density decrease exponentially above $Z_{tangent}$. (*ii*) The background is either the direct source (Sun) or space (which is cold and uniform) unlike the hot and variable surface of the Earth. (*iii*) There is as much as 60-75% more emitting/absorbing material in the limb path than along the nadir path, allowing measurements of temperature and composition to higher altitudes and measurements of gases having lower concentrations.

The disadvantages are: (*i*) Observations are limited to the upper troposphere and above, due to clouds and the finite field-of-view of the instrument. (*ii*) The horizontal resolution is low. (*iii*) It requires precise information about the field-of-view and spacecraft attitude so that the spacecraft pointing can be accurately determined.

4. Retrieval methods

Now, we will address the retrieval problem, *i.e*. how the temperature profile is derived from the measured radiances I_ν at a series of ν. We shall discuss these in general terms, as full solutions are quite complex. So far, we have discussed the RTE that applies to nadir and limb sounding of temperature, and we have introduced the concept of a weighting function. Even under cloud-free conditions, with a noise-free radiometer that measures radiances at all ν, a unique solution for $T(z)$ is not guaranteed. With noise and a limited number of ν, infinite number of solutions are possible. The problem is to find a temperature profile that satisfies the RTE and approximates the true profile as closely as possible. Many approaches are used to solve this problem. They can be roughly grouped into three categories (Rodgers, 1976).

4.1. *Physical retrievals*

These use the forward calculation in an iterative process. To start with, a first guess *(a priori*) temperature profile is chosen. The weighting functions are then calculated. The forward problem (RTE) is solved for the radiance at each ν. If the calculated radiances match the observed radiances within the noise level of the radiometer, then the current temperature profile is accepted. If they do not agree, then the current temperature profile is adjusted and the above steps are repeated. The advantage of such method is that the physical processes are clear at each stage of the retrieval and that no large database of coincident radiosonde data is needed. The disadvantages are that they are computationally expensive, require accurate knowledge of the transmittances τ and do not use known statistical properties of the atmosphere (except in first guess).

Examples: (*i*) *Chahine's Method* - This is a widely used inversion technique that retrieves temperature for as many levels as there are channels in the radiometer. Each temperature corresponds to the peak of the weighting function for a channel. (*ii*) *Smith's Method* - This is also widely used and is similar to Chahine's method. The difference is that the retrieval of temperature is not restricted to be at the same number of levels as there are channels, nor to be at the peaks of the weighting functions. It's a more flexible scheme since the number and height of levels can be chosen, but there will still be only as many independent temperatures as there are channels.

4.2. *Statistical retrievals*

These do not use the RTE directly. Instead, they rely on statistical relationships between ground and space-

based measurements. First of all, a *training data set* of radiosonde temperature profile soundings nearly coincident in time and space with the satellite soundings is compiled. This data set is used to calculate a statistical relationship between the satellite radiances and the radiosonde temperatures. These relationships are then applied to other radiances to retrieve temperature profiles.

The advantages are: (*i*) they are computationally easy, which makes these useful for operational retrievals that must process many radiance measurements (*ii*) they require no knowledge of the transmittances nor use of the RTE (*iii*) they extensively use known statistical properties of the atmosphere. The disadvantages are: (*i*) a large database of coincident radiosonde data is needed for each satellite instrument that should cover all seasons, times of day, latitudes, longitudes, surface types (land, ocean, etc.), and view an area at the same time as the satellite (*ii*) physical processes are embedded in the statistics *e.g*., few radiosondes are launched from high (ground) elevations, so training data sets provide poor coverage of such regions potentially leading to biases in the retrievals.

4.3. *Hybrid retrievals (or inverse matrix methods)*

These combine elements of physical and statistical retrievals. They do not require a large training data set and do use weighting functions. The RTE is first linearized about a standard temperature profile and is converted into a matrix equation. This equation is used to obtain a matrix relating the temperature profile to the radiances, and including the weighting functions. Then several possible approaches can be taken to solve the problem. The advantages are that they are easier to implement than physical or statistical method, include known statistical properties of the atmosphere and no large database of coincident radiosonde data is needed. The disadvantage is that they require accurate knowledge of the transmittances. Optimal estimation is an example of a hybrid method for retrieval of vertical profiles also called the minimum variance or the maximum likelihood method. The formulation of Rodgers (1990) has general applicability, provides an elegant method of combining *a priori* information with measurements and explicitly calculates error on a retrieved profile from the errors in these quantities.

5. Measurements of atmospheric composition

The commonly measured gases are the two most important minor constituents: O_3, and H_2O. Both have a role in determining atmospheric temperature structure and energy balance because they absorb solar and terrestrial radiation. They also play a role in atmospheric chemistry. O_3 absorbs solar UV radiation, which accounts for almost all heating in the stratosphere and also absorbs some IR in the troposphere.

The variation of $\tau_\lambda(z)$, the transmission of the atmosphere from ground to space, with wavelength is shown in Fig. 7, both for the standard atmosphere and each species separately. It can be seen that at 11 μm (atmospheric window), the transmission is unity, the surface term in Equation (2) will dominate giving very nearly the ground temperature. The radiation from Q branch at the center of CO_2 band (667 cm^{-1}) originates at ~240 K, well within the stratosphere. Moving to higher frequencies, absorption coefficient falls and temperature falls to ~220 K characteristic of tropopause, and then rises steadily as the peak of the appropriate weighting function falls in altitude, until 800 cm^{-1} is reached when most of the radiation comes from the surface. Absorption bands for different gases are also given in Table 1 in the IR as well as in the microwave region. Some gases also have absorption features in the ultra violet (such as O_3) and visible (such as O_3, NO_2 etc). In general IR region is preferred for satellite observations since many gases of interest have absorption/emission bands. Effect of scattering by air molecules is much reduced than in the UV or visible region. However, measurements in the IR region have problems if there are clouds. In order to avoid or to reduce this effect, microwave region is more suitable. This region is becoming more useful due to rapid advances in the detector technology and since it is absorbed only if there is precipitable water in the clouds. Many different techniques and instruments are used to measure atmospheric composition. We will concentrate on measurements of ozone. Similar techniques will apply to other trace species except that the wavelength will change according to Fig. 7 and Table 1.

5.1. *Measurements of ozone from satellites*

Ozone has absorption features in all regions of the electromagnetic spectrum (Table 1) and so can be detected using several techniques. Thus there have been 21 satellite experiments to measure ozone before 1980 and many more since then. The three most common techniques use limb or nadir emission (IR or microwave), backscatter ultraviolet (BUV), and solar occultation (UV-visible or IR). A newer technique employs UV-visible limb scattering. A comparison of these techniques can be found in Table 2, while the relevant payloads on various satellites launched so far are given in Table 3. We now discuss below the techniques in details.

5.1.1 *Ozone measurements using emission*

Usually longwave radiation thermally emitted by the atmosphere along the line of sight of the instrument is

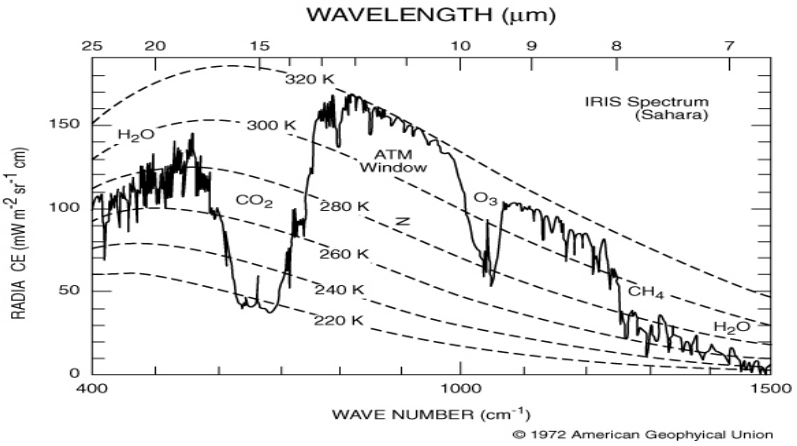

Fig. 7. Examples of thermal emission spectra recorded by IRID D on Nimbus 4. Radiances of black bodies at several temperatures are superimposed. (from Hanel *et al*., 1971)

measured. Measurements can also be made in the infrared (9.6 μm ozone band) or microwave wavelengths. The limb or nadir viewing geometry is commonly used to retrieve ozone profiles and total column, respectively. Instruments in Limb-sounding geometry have a typical vertical resolution of ~3 km. The TOMS instrument uses the earth's emission in the nadir viewing geometry for total column ozone measurements and the results are shown in Figure 1(b). Recall the solution to Schwarzchild's Equation as in nadir sounding of temperature. In this case, T is known so $B(T)$ can be determined. The $d\tau/dy$ term can be derived and used to calculate the unknown mixing ratio of ozone.

5.1.2. *Ozone measurements using UV backscatter*

This is probably the best-known method for the retrieval of ozone from satellite measurements (McPeters, 1984). Here the instrument measures solar UV radiation reflected from the surface and backscattered by the atmosphere or clouds, which is absorbed by ozone in the Hartley-Huggins bands (< 350 nm). Note that most of the ozone lies in the stratosphere but most of the backscattered UV radiation comes from the troposphere. A little absorption by ozone occurs in the troposphere. There is also a little scattering in the stratosphere. The radiation reaching the satellite passes through the ozone layer twice.

The total ozone vertical column is derived as follows. The satellite measures backscattered radiance $I(\lambda) = E_{sun}(\lambda)\ [\tau_{ozone}(\lambda)]^x \times R(\theta_{sun},\theta_{satellite},R_{surface},R_{air})$, where $E_{sun}(\lambda)$ is the solar irradiance at the top of the atmosphere; $[\tau_{ozone}(\lambda)]^x$ is the atmospheric transmission in the ozone band along the slant path, with $\tau_{ozone}(\lambda)$ as the vertical path transmission, $x = \sec\theta_{sun} + \sec\theta_{satellite,}$ the angles being shown in Fig. 8.

$R(\theta_{sun}, \theta_{satellite}, R_{surface}, R_{air})$ is the combined surface-troposphere reflectance which depends on zenith angle, reflection from the surface ($R_{surface}$), and scattering by the air molecules (R_{air}).

Now $\tau_{ozone}(\lambda) = \exp(-\int n\ \sigma_a(\lambda)\ dz) = \exp[-\sigma_a(\lambda)\ U]$, so that if τ_{ozone} can be determined, then total ozone column can be calculated. The difficulty is in determining the reflectance term R. Several satellite instruments measure incoming solar irradiance $E_{sun}(\lambda)$ and backscattered radiance $I(\lambda)$ at two UV wavelengths, one where ozone absorption is strong [$\sigma_a(\lambda)$ is large] and one where ozone absorption is weak) [$\sigma_a(\lambda)$ is small]. Generally, a third observation at λ_3, outside the ozone band, is used to determine the surface term $R_{surface}(\lambda_1) \approx R_{surface}(\lambda_2)$, calculate the Rayleigh scattering term $R_{air}(\lambda)$, and thus determine $R(\lambda_1)$ and $R(\lambda_2)$.

Vertical profiles of ozone can also be derived using the "BUV profiling technique". This relies on the fact that longer the wavelength of the incoming UV irradiance, the weaker the ozone absorption and so the lower (in height) the penetration of the UV light into the atmosphere. The absorption increases with decreasing wavelength, such that radiation at progressively shorter wavelengths is significantly absorbed at progressively higher altitudes. So the backscattered radiation at specific UV wavelengths can only be scattered from above a particular height. Below this level, all the radiation is absorbed and there is no backscattered radiance. Measurements at certain UV wavelengths are sensitive to specific portions of the ozone vertical profile, and the full profile can be obtained by measuring radiation at a series of wavelengths and using a retrieval algorithm that converts each radiance measurement to and atmospheric quantity.

TABLE 2

Advantages and disadvantages of the four measurement techniques (source: Strong, 2002)

Technique	Advantages	Disadvantages
Emission	• doesn't require sunlight	• slightly less accurate than backscatter UV
	• long time series	• long horizontal path for limb observations
	• simple retrieval technique	
	• good spatial coverage	
Backscatter	• accurate	• requires sunlight–cannot be used over winter poles
UV	• long time series	• poor vertical resolution below O_3 peak (~30 km)
	• good horizontal resolution Due to nadir viewing	due to the effects of multiple scattering and reduced sensitivity to the profile shape.
Occultation	• simple equipment	• can only be made at satellite sunrise and sunset, which
	• simple retrieval technique	limits the number and location of measurements
	• good vertical resolution	• long horizontal path
	• self-calibrating	
Limb	• excellent spatial coverage	• complex viewing geometry
Scattering	• good vertical resolution	• poor horizontal resolution
	• data can be taken nearly continuously	

5.1.3. *Ozone measurements using occultation*

This is probably the simplest method for the retrieval of ozone profiles from satellites (Russell *et al.,* 1994). Here the atmospheric extinction at a UV-visible or infrared wavelength sensitive to ozone absorption is measured from a satellite as the Sun, Moon, or a star rises or sets. Disadvantage of the use of stars is that measurements may not go as low in the atmosphere as solar occultation. The extinction through the limb of the atmosphere is measured as a function of tangent height, allowing the optical mass to be determined. The vertical resolution is typically 1-2 km, which is better than the BUV profiling technique. A representative measurement scenario is depicted in Fig. 1(a), which covers a latitude belt from 50°S to 50°N and 100 hPa to 0.05 hPa (≈ 15 - 70 km height range).

Let us define $I_\lambda(0)$ = intensity at the highest altitude where ozone extinction is zero and $I_\lambda(z_i)$ = intensity measured at the i-th tangent height z_i. Their ratio is a measure of the transmittance $\tau_\lambda(z_i)=I_\lambda(z_i)/I_\lambda(0) = \exp(-\int\sigma_{ext,\lambda}(s)\,ds)$. The term in the exponential is related to the total ozone column U, as in the section above. By measuring $\tau_\lambda(z_i)$ for a series of tangent heights, a set of columns, $U(z_i)$can be calculated and then inverted to get the ozone vertical profile. Note that the same instrument is used to measure the attenuated and unattenuated radiation, so any long-term instrument changes disappear when the ratio is calculated. This is why occultation instruments are often called self-calibrating. Main disadvantage is that observations are made as the source (usually Sun) rises or sets relative to the satellite. Also, the concentration of some gases changes rapidly during twilight, which can make it difficult to interpret measurements over the long horizontal limb path.

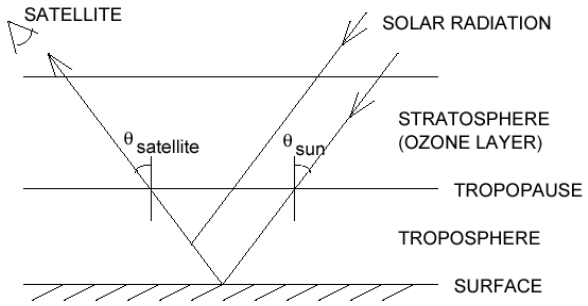

Fig. 8. Measurement of O_3 using backscattered UV (source : Strong, 2002)

5.1.4. *Ozone measurements using limb scattering*

This is a newer technique that combines some of the features of the first three (Waters *et al*., 1998). It has been previously used, but the altitude range was limited to the upper stratosphere and mesosphere. It is now of interest for the upper troposphere and lower stratosphere, since the measurements from this region could significantly improve the top boundary conditions of tropospheric chemistry-transport models. The viewing geometry is similar to that of both limb emission and occultation, which provides good vertical resolution. The instrument measures scattered solar radiation in a manner similar to

TABLE 3

Instruments launched on satellites till date, using various measurement techniques

+Payload	Satellite	Year	Technique	Species measured	Ref.
LIMS (Limb IR Monitor of the Stratosphere)	Nimbus 7	1978-79	Limb sounding (emission) (6-channel filter radiometer in 6-15 μm band)	O_3, HNO_3, H_2O, NO_2	Russell *et al*. 1984
SBUV (Solar Backscatter UV)	Nimbus-7	1978-90	UV Backscatter, $\lambda_1,\lambda_2, \lambda_3$	O_3	McPeters *et al*. 1984
TOMS	Nimbus 7 Meteor 3 ADEOS Earth Probe	1978-93 1991-94 1997 1996	UV Backscatter : 3 pairs-313/331, 318/331, 331/340 nm, global maps once a day	Total ozone columns	Stolarski *et al*.. 1991
SAGE-II (Stratospheric Aerosol & Gas Experiment)	Earth Radiation Budget Satellite (ERBS)	1984	Solar occultation; solar attenuation by atmosphere's limb as sun rises/sets relative to spacecraft, in 7 bands (90.386-1.02 μm).	O_3 (Chappuis band at 0.6 μm) NO_2, H_2O,aerosols (UV, visible channels)	McCormick *et al*. 1992
HALOE	UARS	1991	IR solar occultation using gas correlation cells and broadband channels	O_3, HCl, HF, CH_4, H_2O, NO, NO_2, aersol	Russell *et al*. 1994
ISAMS (Improved SAMS)	UARS	1991-92	IR limb emission using pressure modulated radiometers	O_3,CH_4,CO,H_2O,NO,N_2O, HNO_3,N_2O_5,aerosol	Connor *et al*.. 1996
MLS (Microwave Limb Sounder)	UARS	1991	Microwave limb emission using heterodyne spectroscopy	O_3, ClO, H_2O, and T	Waters 1998
CLAES (Cryogenic Limb Array Etalon Spectrometer)	UARS	1992-93	IR for limb emission using a Fabry-Perot interferometer	N_2O, CFC-11, CFC-12, CH_4, H_2O, NO, NO_2, HNO_3, HCl, N_2O_5, CO_2	Roche *et al*. 1993
GOME (Global Ozone Monitoring Experiment)	ERS-2 (European Remote Sens. Sat.	1995	Nadir-viewing BUV technique, measures radiances from 240-793 nm. 2 days to create a global map	O_3 column & profiles, columns of NO_2, H_2O, SO_2, BrO, OClO	Burrows *et al*. 1999
MOPITT	NASA Terra	1999	Nadir (4.6 & 2.3 mm band for CO, 2.2 mm for CH_4)	CH_4 cols., CO cols and profiles	Edwards *et al.* 1999
GOMOS (Global Ozone Monitoring by Occultation of Stars)	ENVISAT	2001	Stellar occultation in UV-visible	O_3, NO_2, NO_3 profiles	Bertaux *et al*. 1991
SCIAMACHY	ENVISAT	2002	Both nadir and limb scanning. Measures transmitted, back scattered, and reflected radiation in range 240-2400 nm	O_3, H_2O, CO, NO_2, CH_4 in troposphere and stratosphere	Bovensmann *et al*. (1999)

BUV, but the light source is in earth's limb. This technique provides coverage through the atmosphere, and hence good column measurements can also be made.

Equation for limb radiance I, at wavelength λ and tangent height z_{tan}, contains an integral of the transmittance along the line-of-sight. It can be broken down into two terms, corresponding to solar irradiance incident on the atmosphere beyond the tangent point and between the tangent point and the satellite, as illustrated below for a scattering angle of 90 (Fig. 9). Vertical profiles of concentration can be retrieved from

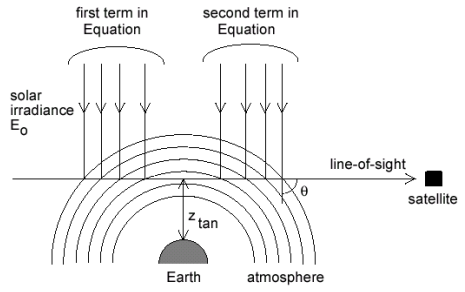

Fig. 9. Geometry for observations using limb scattering (source : Strong, 2002)

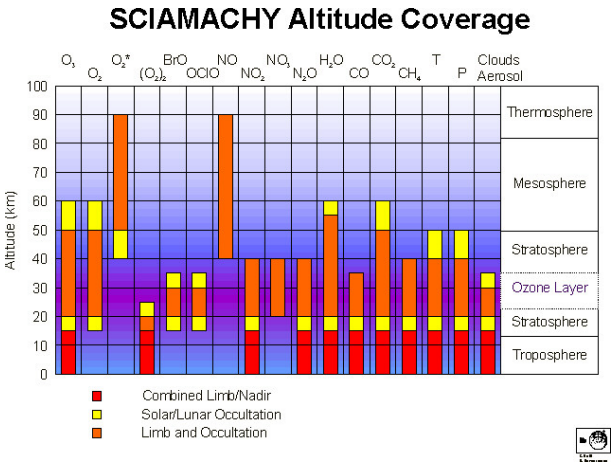

Fig. 10. Diagram showing typical altitude range and the species measured by SCIMACHY (Scanning Imaging Absorption SpectroMeter for Atmospheric CHartographY) (http://envisat.esa.int/instruments/sciamachy/index.html)

UV-visible limb radiance spectra by using a radiative transfer model to simulate the measurements and derive a set of weighting functions. These can then be incorporated into an inversion scheme, such as optimal estimation to derive the trace gas profiles.

On the other hand the new generation instruments are able to maneuver at both viewing geometries such as limb, including sun and moon occultation, covering the wavelength range extending to the near IR region (apart from the UV/Visible wavelength range of 240 nm to 800 nm). Therefore, this experiment is expected to put forward a challenge for optimal use of available information in terms of radiative transfer modeling (*e.g.* extension to limb/occultation geometries and to infrared wavelength region) and retrieval algorithms such as global fitting for limb and occultation geometries, combination of limb and nadir measurements, height-resolved retrieval form nadir measurements for some gases. The SCIAMACHY altitude coverage of trace gases measurements and complexities involved in their retrievals are depicted in Fig. 10.

6. Conclusions

Since the satellite observations are often targeted for global coverage, lesser measurement accuracy is generally acceptable due to difficulties associated with instrumental operation and retrieval algorithms. In fact, no other mode of measurements can match with the satellite measurements due to global measurements over a long period. In 2004, NASA will launch the Earth Observing System (EOS) Aura (http://eos-chem.gsfc.nasa.gov) which will carry a number of instruments to measure O_3, H_2O, CH_4 etc. In 2005, SMILES (Superconducting sub mm Wave Limb Emission Sounder) will be launched on the Japanese Experimental Module (JEM) of the International Space Station (ISS). On the other hand, the Asian region (mainly India and China) has the highest economic growth rate and will continue for some period. This is leading to increased emissions of various gases and aerosols into the atmosphere. There is a need for satellite borne measurements of atmospheric constituents like aerosol, ozone, CO, water vapour and other gases which directly or indirectly could alter the radiative balance of the atmosphere or the chemical composition which may affect human life, crop yields, forest cover etc in this region. A satellite in low inclination orbit will probably be best suitable for this purpose as the frequency of measurements at a particular place is higher than a polar orbit satellite. A geostationary satellite, which will keep a watch on pollution and meteorological events round the clock, will also be suitable.

References

Bertaux, J. L., Megie, G., Widemann, T., Chassefiere, E., Pellinen, R., Kyrölä, E., Korpela, S. and Simon, P., 1991, "Monitoring of Ozone Trend by Stellar Occultations : The GOMOS Instrument", *Adv. Space Res*., **11**, 237-242.

Bovensmann, H, Burrows, J. P., Buchwitz, M., Frerick, J., Noël, S., Rozanov, V. V., Chance, K. V. and Goede, A. H. P., 1999, "SCIAMACHY - Mission objectives and measurement modes", *J. Atmos. Sci*., **56**, 127-150.

Brasseur, G. and Solomon, S., 1986, "Aeronomy of the middle atmosphere", D. Reidel Publishing Co., Dordrecht, 2nd Ed., p452 .

Burrows, J. P., Weber, M., Buchwitz, M., Rozanov, V., Ladstaetter-Weissenmayer, A., Richter, A. and Eisinger, M., 1999, "The Global Ozone Monitoring Experiment (GOME): Mission Concept and First Scientific Results", *J. Atm .Sci.,* **56**, 151-175.

Connor, B. J., Scheuer, C. J., Chu, D. A., Remedios, J. J., Grainger, R. G., Rodgers, C. D. and Taylor, F. W., 1996, "Ozone in the Middle Atmosphere as Measured by the Improved Stratospheric and Mesospheric Sounder,", *J. Geophys. Res.,* **101**, 9831-9842.

Crutzen, P. J., 1970, "The influence of nitrogen oxide on the atmospheric ozone content", *Quart. J. Roy. Met. Soc*., **96**, 320-325.

Dessler, A. E., Burrage, M. D., Grooss, J. U., Holton, J. R., Lean, J. L., Massie, S. T., Schoeberl, M. R., Douglass, A. R. and Jackman, C. H., 1998, "Selected science highlights from the first 5 years of the upper atmosphere research satellite (UARS) program", *Rev. Geophys*., **36**, 183-210.

Edwards, D. P., Halvorson, C. M., and Gille, J. C., 1999, "Radiative transfer modeling or the EOS Terra satellite Measurement of Pollution in the Troposphere (MOPITT) instrument", *J. Geophys. Res*., **104**, 16755.

Farman, J. C., Gardiner B. G. and Shanklin, J. D., 1985, "Large losses in total ozone in Antarctica reveals ClOx/NOx interaction", *Nature,* **315**, 207-210.

Fishman, J., Fakhruzzaman, K., Cros, B. and Nganga, D., 1991, "Identification of widespread pollution in the Southern Hemisphere deduced from satellite analyses", *Science*, **252**, 1693-1696.

Garcia, R. R. and Solomon, S., 1983, "A numerical model of zonally averaged dynamical and chemical structure of the middle atmosphere", *J. Geophys. Res*., **88**, 1379-1400.

Hanel, R. A., Schlachman, B., Rogers, D. and Vanous, D, 1971, "Nimbus-4 Michelson Interferometer", *Applied Optics*. **10**, 1376-1382.

Hofmann, D. J., Oltmans, S. J. , Lathrop, J. A., Harris, J. M. and Vomel, H., 1994, "Record low ozone at the South Pole in the spring of 1993", *Geophys. Res. Lett*., **21**, 421-424.

Houghton, J. T., Taylor F. W. and Rodgers, C. D., 1984, "Remote sounding of atmospheres", Cambridge University Press., Cambridge, U.K., p343 .

Hudson, R. D. and Thompson, A. M., 1998, "Tropical tropospheric ozone from total ozone mapping spectrometer by a modified residual method", *J. Geophys. Res.,* **103,** 22129-22145.

Jones, R. L. and Pyle, J. A., 1984, "Observations of CH_4 and N_2O by the Nimbus 7 SAMS: a comparison with *in situ* data and two-dimensional numerical model calculations", *J. Geophys. Res*., **89**, 5263-5279.

Lal, S., Acharya, Y. B., Patra, P. K., Rajaratnam, P., Subbaraya, B. H. and Venkataramani, S., 1996, "Balloon-borne cryogenic air sampler experiment for the study of atmospheric trace gases", *Indian J. Radio Space Phys*., **25,** 1-7.

Lal, S., Naja, M. and Jayaraman, A., 1998, "Ozone in the marine boundary layer over the tropical Indian Ocean", *J. Geophys. Res*., **103**, 18907-18917.

Lal, S., Naja M. and Subbaraya, B. H., 2000, "Seasonal variations in surface ozone and it's precursors over an urban site in India", *Atmos. Env*., **34**, 2713-2724.

McCormick, M. P., Veiga, R. E. and Chu, W. P., 1992, "Stratospheric ozone profile and total ozone trends derived from the SAGE I and SAGE II data", *Geophys. Res. Lett*., **19**, 269-272.

McPeters, R. D., Heath, D. F. and Bhartia, P. K., 1984, "Average ozone profiles for 1979 from the NIMBUS 7 SBUV instrument", *J. Geophys. Res*., **89**, 5199-5214.

Molina, J. S. and Rowland, F. S., 1974, "Stratospheric sink for chlofluoromethanes: Chlorine atom-catalized destruction of ozone", *Nature*, **249**, 810-812.

Naja, M. and Lal, S., 1996, "Changes in surface ozone amount and it's diurnal and seasonal patterns from 1954-55 to 1991-93, measured at Ahmedabad (23N, India)". *Geophys. Res. Lett*., **23**, 81-84.

Patra, P. K. and Santhanam, M. S., 2002, "Three Dimensional Analysis of HALOE CH_4: Implications of Stratosphere-Mesosphere Dynamics", *submitted to Annales Geophys.*

Patra, P. K. and Maksyutov, S., 2002, "Incremental approach to the optimal network design for CO_2 surface source inversion", *Geophys. Res. Lett*., in press (10.1029/2001GL013943).

Patra, P. K., Maksyutov, S. and Santhanam, M. S., 2002, "Derived trends of CH_4 in the stratosphere from HALOE measurements", in Proc. Non-CO_2 Greenhouse Gases: Scientific Understanding, control and implementation, Allenpress, Netherlands (in press).

Patra, P. K., Lal, S. Chand, D., Venkataramani, S., 2002a, "HALOE and balloon-borne measurements of methane in the stratosphere and their relation to QBO", submitted to *J. Atmos. Sci*.

Ramanathan, V., Cicerone, R. J., Singh, H. B. and Kiehl, J. T., 1985, "Trace gas trends and their potential role in climate change", *J. Geophys. Res*., **90**, 5547-5566.

Roche, A.E., Kumer, J.B., Mergenthaler, J..L., Ely, G.A., Uplinger, W.G., Potter, J.F., James, T.C. and Sterritt, L.W., 1993, "The Cryogenic Limb Array Etalon Spectrometer (CLAES) on UARS: Experiment Description and Performance," *J. Geophys. Res*., **98**, 10763-10775.

Rodgers, C. D., 1976, "Retrieval of atmospheric temperature and composition from remote measurements of thermal radiation", *Rev. Geophys. Sp. Phys*., **14,** 609-624.

Rodgers, C. D., 1990, "Characterization and error analysis of profiles retrieved from remote sounding measurements", *J. Geophys. Res*., **95**, 5587-5595.

Russell, J. M., Gille, J. C., Remsberg, E. E., Gordley, L. L., Bailey, P. L., Fisher, H., Girard, A., Drayson, S. R., Evans W. F. J. and Harries, J. E., 1984, "Validation of Water Vapour Results Measured by the Limb Infrared Monitor of the Stratosphere (LIMS) experiment on Nimbus-7", *J. Geophys. Res*., **89**, 5115-5124.

Russell, J. M., III, Gordley, L. L., Deaver, L. E., Thompson, R. E. and Park, J. H., 1994, "An overview of the Halogen Occultation Experiment (HALOE) and preliminary results," *Adv. in Space Res*., **14**, 9-13.

Stolarski, R. S., Bloomfield, P., McPeters, R. D. and Herman, J. R., 1991, "Total ozone trends deduced from Nimbus-7 TOMS data", *Geophys. Res. Lett.,* **18**, 1015-1018.

Strong, K., 2002, "Earth Observations from Space - Lecture notes of course PHY 499S offered at the University of Toronto, Canada".

Subbaraya, B. H., 1987, Vertical distribution of minor constituents in the tropical middle atmosphere, *Ind. J. Radio Space Phys*., **16**, 25-25.

Waters, J. W., 1998, "Atmospheric measurements by the MLS experiments: Results from UARS and plans for the future", *Adv. Space Res*., **21**, 1363-1372.

World Meterological Organization (WMO), 1995, "Scientific assessment of ozone depletion: 1994", *Global Ozone Res. Monit. Proj., WMO Rep*. **37**, Geneva.

Yates, H. W., 1972, "Remote Sensing from Satellites", in "Remote sensing of the troposphere", V.E. Derr, ed., NOAA, 26.1-26.44.

Ziemke, J. R., Chandra, S., and Bhartia, P. K., 1998, Two new methods for deriving tropospheric column ozone from TOMS measurements: Assimilated UARS MLS/HALOE and cenvective-cloud differential techniques, *J. Geophys. Res*., **103**, 22,115-22,127.